Available online at www.sciencedirect.com

ScienceDirect

Procedia Engineering 10 (2011) 25–30

Engineering Procedia

ICM11

Dynamic Debonding Strength of Fiber Glass Composite

Fergyanto E. Gunawan*

Department of Industrial Engineering, Binus University, Jl. K. H. Syahdan 9, Jakarta 11480, Indonesia

Abstract

A laminated composite may fail by various mechanisms: debonding, delamination, fiber fracture, matrix cracking, and fiber buckling. The fiber fracture possess the greatest threat the structure integrity. However, the progressive debonding often increases the load sustained by the fiber; therefore, it may promote the fiber fracture. It is clear that data of the debonding strength are crucial. Unfortunately, the experiment for the purpose is often difficult particularly in a high-strain rate case. In this paper, we present an experimental technique to obtain the mechanical properties of the debonding in the high-strain rate case.

Keywords: Cohesize zone model, dynamic debonding, fracture mechanics, finite element analysis

1. Introduction

Debonding is a prominent fracture mechanism particularly in a long fiber reinforced composite structure. Therefore, characterizing the debonding properties such as the strength and the fracture energy is essential.

Many systematic investigations [1--17] have been performed to study the debonding despite existence of many challenges particularly in the experimental aspects. Within this respect, one major issue is related with the specimen design. The specimen should allow one to easily produce the debonding on various loading conditions, to easily observe the debonding process, and to easily measure parameters related to the debonding.

The experiments in studying the debonding phenomenon can mainly be divided into two groups: the fiber pull-out testing method and the fiber push-out testing method. The fiber pull-out test particularly

* Corresponding author. Tel.: (+62 - 21) 534 - 5830; fax: (+62 - 21) 530 - 0244.
E-mail address: fgunawan@binus.edu

1877-7058 © 2011 Published by Elsevier Ltd. Open access under CC BY-NC-ND license.
Selection and peer-review under responsibility of ICM11 doi:10.1016/j.proeng.2011.04.006

using a single fiber has been widely used with great success [1, 5, 9, 10] on various conditions such as on a transversal loading condition [8], and on a microscopic condition using a drop of the matrix as called the microbond test method [6, 9, 10]. In addition, the method has also been studied analytically [16] by taking into account the friction effect [3,4], the thermal stress, and the residual stress [11]. Not only using a single fiber, the pull-out testing method has also been used in the debonding involving a bundle of fibers [2, 12, 15, 17]. The use of a bundle instead of a single fiber is particularly interesting when dealing with a very small fiber diameter such as natural fibers. The kenaf natural fiber, for an example, only has a diameter in range of 40--70 [18]. Even in an experiment involving an synthetic fiber, Ref. [14] suggested that using a bundled fibers allowed a better control and better visualization of the failure process. Therefore, a debonding test using a bundle of fibers is easier in a number of circumstances. In addition to the fiber pull-out testing method, the debonding phenomenon has also been studied by means of the fiber push-out testing method [7, 13, 14]. Reference [7] has provided a theoretical analyses of the method, on the basis of the fracture mechanics, and has also compared the results to those of the fiber pull-out method. The fiber push-out method seems to offer a simple technique to study the debonding in dynamic loading conditions, specifically in conjunction with the Hopkinson testing method [13, 14].

In this work, we present a specimen design, which in combination with the numerical model of the debonding of Xu and Needleman [19], allows us to infer the debonding characteristics in a high strain rate regime by means of the Hopkinson bar testing apparatus [20].

2. Debonding Specimen and Its Numerical Model

2.1. The Specimen Design

To measure the debonding strength in the static and the dynamic loading conditions, we devised a cylindrical-type specimen as shown in Fig. 1.

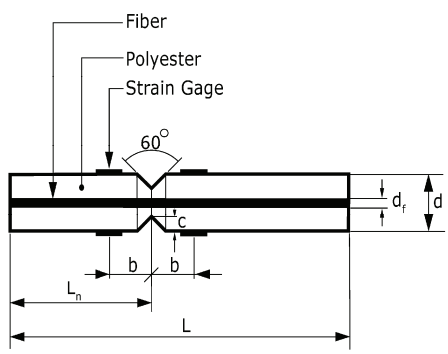

Figure 1: Geometry of the debonding specimen

The specimen has a bundle of glass fibers that placed along its axis strengthened by the epoxy material. Two types of the specimens were produced: 1 mm and 2 mm of the bundle diameter. The specimen length for the dynamic test was 200 mm; It was designed such that the incident wave could clearly be separated from the reflected wave. A shorter specimen was used in a static test. The specimen was simply manufactured in the laboratory by using a 10 mm diameter aluminum tube. The specimen diameter was reduced to 9.5 mm using a lathe machine; and a notch having an angle of 60 degree was introduced to the

specimen. On each specimen, four strain gages were attached at a distance of 20 mm from the notch. The mechanical properties of the glass fiber are 76.0 GPa for the Young's modulus, 0.23 for the Poisson's ratio, and 1165 kg/m^3 for density; meanwhile, for the hardened polyester, these properties are 5.4 GPa, 0.32, and 2450 kg/m^3.

2.2. The Finite Element Model of the Debonding Specimen

For the above specimen design, the debonding properties cannot be inferred directly from the test data, but indirectly by means of a finite element analysis. Figure 2 shows the detailed finite element mesh of the debonding specimen. The specimen was assumed to be axis-symmetric. The most important features of the model were the zero thickness cohesive elements [21]. Those elements were introduced to the model such the observed debonding on the specimen (see Fig 3) could be reproduced. The debonding on the specimen was produced by means of the Hopkinson bar testing apparatus [20].

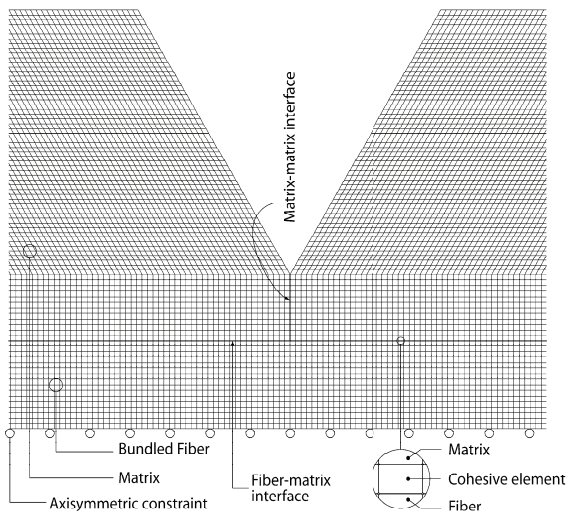

Figure 2: The finite element model of the debonding specimen of Fig. 1

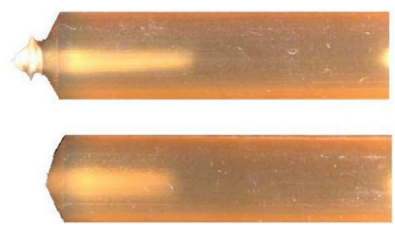

Figure 3: The debonding specimen

In the model of Fig. 3, it was assumed that the crack would start from the notch root, and then straightly propagate to the fiber-matrix interface although in the experiment, it was not always straight. Furthermore, it was also assumed that the traction-separation model of the cohesive elements following the bilinear softening model [21, 22] and its mechanical properties were governed by the elastic modulus, the material strength, and the interface fracture energy. In this particular model, the debonding would be initiated when the following is satisfied:

$$\left(\frac{\langle T_n \rangle}{T_n^c}\right)^2 + \left(\frac{T_s}{T_s^c}\right)^2 = 1$$

where $\langle \quad \rangle$ is the Macaulay brackets that set any negative values to zero, T denotes the traction or the material strength, the subscript n denotes for the normal direction, the subscript s denotes for the shear direction, and the superscript c denotes the critical value. However, complete debonding only occurs when

$$\left(\frac{G_n}{G_n^c}\right)^{\alpha} + \left(\frac{G_s}{G_s^c}\right)^{\alpha} = 1$$

In the above equation, G denotes the cohesive energy, and $\alpha = 1$ is suitable for the thermoplastic matrix composites [23].

2.3. The Model Calibration and Results

The identification of the cohesive zone model's parameters were performed in two steps. Those parameters related to the cohesive zone model in the matrix-matrix interface were established in the first step, and followed by the calibration for the parameters of the fiber-matrix interface. The calibration of those material parameters were completely performed on the basis of the data obtained from the tests of the 1 mm fiber-bundle specimens; then, the established model was used to predict the debonding propagation on the 2~mm fiber-bundle specimen. The calibration results: for the matrix-matrix interface, the tensile strength was 72 MPa, and the critical cohesive energy in tension was 2 MPa·mm; for the fiber-matrix interface: the tensile strength was 54 MPa the shear strength was 67 MPa, and the critical cohesive energy was 2 MPa·mm for the both modes. Although a dominant mixed mode fracture occurred on the fiber-matrix interface, but the matrix-matrix interface fractured in a pure normal mode. In Fig. 4 to Fig. 7, we compare the experimental data with the data predicted by the model.

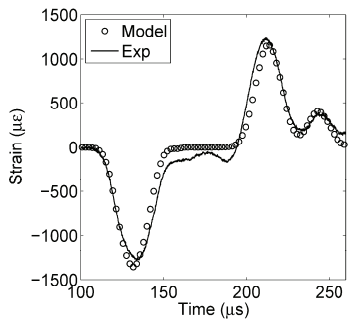

Figure 4: The solid line is the strain-time history recorded at the rear-gage of the 1 mm bundled fiber diameter specimen when the matrix ahead of the notch fractured, and the circle denotes the simulation results.

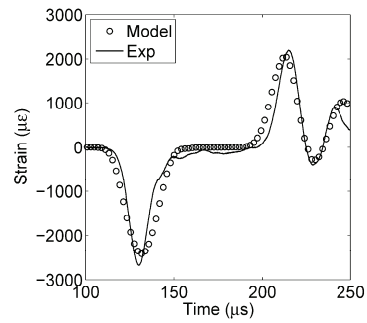

Figure 5: The solid line is the strain-time history recorded at the rear-gage of the 1~mm bundled fiber diameter specimen when the debonding on the matrix-fiber interface was about to occur, the circle denotes the simulation results.

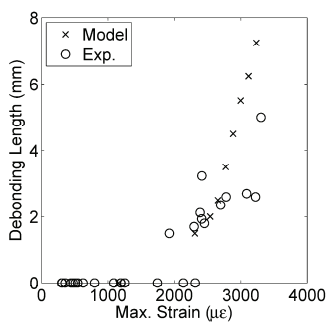

Figure 6: The maximum strain of the reflected stress-wave at the rear gage versus the debonding length of 1 mm bundled fiber diameter specimen.

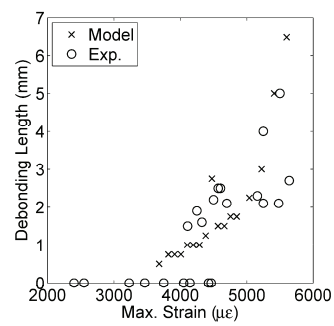

Figure 7: The maximum strain of the reflected stress-wave at the rear gage versus the debonding length of 2 mm bundled fiber diameter specimen.

3. Discussion

We first discuss comparisons of the model predictions and the experimental data from a macroscopic level and then from a microscopic level. At the end, we discuss the mode mixity of the debonding-tip during propagation.

In the macroscopic level, we compare the strain time history recorded in the experiment to those predicted by the model. Only the case of 1 mm bundle-fiber specimen is presented in this paper due limitation of the space. Figure 4 shows a comparison when the matrix ahead of the notch fractured; meanwhile, Fig. 5 shows a comparison when the debonding has also occurred on the interface. In general, those figures show that the model reasonably reproduced the data recorded in the experiment particularly along the time of the stress wave reached the measurement point; however, during the unloading, significant deviation exists between the two, but this clearly due to the error in the experimental data. Rather similar nature were also observed for the case of 2 mm bundle-fiber specimen. Hence, we conclude the model is acceptable in the macroscopic level.

In the microscopic level, we compare the debonding length obtained in the experiments to those predicted by the model. For the two-type of specimens, the results are reproduced in Fig. 6 for the 1 mm bundle-fiber specimen and in Fig. 7 for the 2 mm bundle-fiber specimen. We should note that the maximum strains in the figures are those associated with the reflected tensile stress-waves. In this comparison, unlike the comparison of the strain-time history, reasonable deviations existed between those two data. The deviations were mainly due to scattering of the maximum strain and debonding length data obtained from the experiments; meanwhile, the relation between the maximum strain and the debonding length obtained from the model was more consistent. However, from a statistical point of view, the experimental data seems to scatter around the model predicted data within an acceptable band. Therefore, the model also reasonably reproduced the experimental data in the microscopic level.

The crack was initiated at the notch root, then propagated to the interface, and finally, kinked to the left and the right on the interface. The tensile stress-wave reached the notch around 136.8 μs, and instantly, initiated debonding on the interface. Initially, the normal component was slightly bigger than the tangential component; but the tangential component quickly increased. At a certain debonding length, the mode mixity became a constant, and the debonding mainly propagated at the case.

4. Conclusion

In conjunction with the numerical model of the debonding of Xu and Needleman [19], we have proposed an experimental design that allows us to characterize the debonding properties. In this particular design, when the debonding is reasonably long, the debonding propagates at a constant mode mixity on the dynamic loading condition as well as on the static loading condition [15], but a different mode mixity can easily be obtained by changing the radius ratio of the fiber and the matrix. Since the debonding characteristics strongly depend on the mode mixity [24] the current specimen would allow one to obtain easily the debonding characteristics for a wide range of the mode mixity.

Acknowledgments

I thank Fenny T. Kurniawati and Motoharu Yamauchi for performing the debonding test statically and dynamically during their studentship at Toyohashi University of Technology in Japan.

References

[1] J.-P. Favre, M.-C. Merienne, Characterization of fibre/resin bonding in composites using a pull-out test, International Journal of Adhesion and Adhesives 1(6) (1981) 311- 316. http://dx.doi.org/DOI: 10.1016/0143-7496(81)90025-7

[2] J.K. Wells, P.W.R. Beaumont, Debonding and pull-out processes in fibrous composites, J. of mat. sci. 20 (1985) 1275--1284.

[3] A.A.G. Evans, M.Y. He, J.W. Hutchinson, Interface debonding and fiber cracking in brittle matrix composites, Journal of the American Ceramic Society 72 (12) (1989) 2300--2303.

[4] J. W. Hutchinson, H. M. Jensen, Models of fiber debonding and pullout in brittle composites with friction, Mechanics of materials 9 (1990) 139--163.

[5] J. K. Kim, C. Baillie, Y. W. Mai, Interfacial debonding and fiber pull-out stresses---part 1: Critical comparison of existing theories with experiments, Journal of materials science 27 (1991) 3143--3154.

[6] L.P. Hann, D.E. Hirt, Simulating the microbon technique with macrodroplets, Composites sci. and tech. 54 (1995) 423--430.

[7] L.M. Zhou, Y.W. Mai, L.Ye, Analyses of fiber push-out test based on the fracture mechanics approach, Composites Engineering 5 (10--11) (1995) 1199--1219.

[8] H. Zhang, M. L. Ericson, J. Varna, L. A. Berglund, Transverse single-fiber test for interfacial debonding in composites: 1. experimental observations, Composites Part A 28A (1997) 309--315.

[9] T. Schuller, W. Becker, B. Lauke, Analytical and numerical calculation of the energy release rate for the micro bond test, The journal of adhesion 70 (1999) 33--56.

[10] C. H. Liu, J. A. Naim, Analytical and experimental methods for a fracture mechanics interpretation of the micro bond test including the effect of friction and thermal stresses, International journal of adhesion and adhesives 19 (1999) 59--70.

[11] J. A. Nairn, C. H. Liu, D. A. Mendels, S. Zhandarov, Fracture mechanics analysis of the single-fiber pull-out test and the microbon test including the effect of friction and thermal stresses, in: Proceeding 16th annual technology conference of the american society of composites, 2001.

[12] F. E. Gunawan, H. Homma, N. Yamauchi, F. T. Kurniawati, Dynamic interface debonding between a glass fiber bundle and a matrix, in: Proceeding of the 2002 annual meeting of JSME/MMD, Yamaguchi, Japan, 2002, pp. 667--668.

[13] Z. Li, X. Bi, J. Lambros, P. H. Geubelle, Dynamic fiber debonding and frictional push-out in model composites systems: experimental observations, Experimental mechanics 42 (3) (2002) 417--425.

[14] X. Bi, Z. Li, P. H. Geubelle, J. Lambros, Dynamic fiber debonding and frictional push-out in model composite systems: numerical simulations, Mechanics of Materials 34 (2002) 433--446.

[15] F. E. Gunawan, H. Homma, F. T. Kurniawati, M. Yamauchi, Static debonding initiation stress of fiber glass composite, JSME International journal, Series A 47 (2) (2004) 122--129.

[16] N. A. Noda, R. Shirao, J. Li, J. S. Sugimoto, Intensity of singular stress fields causing interfacial debonding at the end of a fiber under pullout force and transverse tension, International journal of solid and structures 44 (2007) 4472--4491.

[17] F. E. Gunawan, H. Homma, S. Shirley, An analysis of debonding along interface of bundled fibers and matrix, Journal of solid mechanics and materials engineering 2 (2008) 310--318.

[18] Y. Xue, Y. Du, S. Elder, D. Sham, M. Horstemeyer, J. Zhang, Statistical tensile properties of kenaf fibers and its composites, in: 9th International conference on wood and biofiber plastic composites, 2007.

[19] X. P. Xu, A. Needleman, Numerical simulation of dynamic crack growth along an interface, International journal of fracture 74 (1996) 289--324.

[20] H. Kolsky, Stress Waves in Solids, Dover Publication, Inc., New York, 1963.

[21] ABAQUS Analysis User's Manual Version 6.8.

[22] P. H. Geubelle, J. Baylor, The impact-induced delamination of laminated composites: A 2d simulation, Composites, Part~B 29B (1998) 589--602.

[23] P. P. Camanho, C. G. Davila, Mixed-mode decohesion finite elements for the simulation of delamination in composite materials, Tech. Rep. NASA/TM-2002-211737, NASA Langley Research Center, Hampton, VA 23681-2199 (June 2002).

[24] W. Yang, Z. Sui, C. F. Shih, Mechanics of dynamic debonding, Proc. Royal Society London A 433 (1991) 679--697.